

Magnetic properties of MnF_2 and CoF_2 determined by implanted positive muons. II. Sublattice magnetization and phase transition

R. De Renzi, G. Guidi, P. Podini, and R. Tedeschi

Department of Physics, University of Parma, I-43100 Parma, Italy

C. Bucci

Department of Physics, University of Parma, I-43100 Parma, Italy

and Experimental Physics Division, European Organization for Nuclear Research (CERN), CH-1211 Geneva 23, Switzerland

S. F. J. Cox

Rutherford Appleton Laboratory, Chilton, Oxfordshire OX11 0QX, United Kingdom

(Received 6 December 1983)

Since it has been established in a companion paper that implanted positive muons occupy well-defined interstitial positions in CoF_2 and MnF_2 , it has been possible to measure the sublattice magnetization and the critical spin fluctuations near T_N which are reported in this paper. In CoF_2 , below the Néel temperature, the muon-spin-rotation (μSR) experiments in the absence of external fields reveal a signal whose frequency is proportional to the spontaneous sublattice magnetization. Its temperature dependence clearly reflects the presence of the strong magnetic anisotropy. In particular at the lower temperatures the behavior follows the predictions of spin-wave theory, while on approaching T_N a simple power-law dependence agrees with the three-dimensional Ising model. The linewidths of the μSR signal in the neighborhood of T_N in both crystals display a critical broadening which again can be asymptotically described by power laws. Such data are analyzed and critically compared with existing NMR and neutron scattering experiments. In this respect, our data reveal the anisotropy crossover in MnF_2 and the existence of a central diffusive peak in the scattering function of CoF_2 , below T_N .

I. INTRODUCTION

Since the early applications of μSR to the study of crystalline materials, magnetism has been a natural test field for the characterization of the muon as a probe of the local or "hyperfine" fields.¹ After the initial interest in magnetic metals, recently, attention has been given to magnetic insulators, where the "local" fields are expected to be free from the complication of a contact interaction with conduction electrons.

In this context, magnetic oxides,²⁻⁴ antiferromagnetic insulators,⁵ and ferrimagnetic systems^{6,7} have been studied in some detail, and it has been established that the local fields measured at the muon site(s) can be correlated with the magnetic properties of the systems. Two important features concerning muons, however, are particularly relevant when studying insulating magnetic materials: the first concerns the dynamic state of the muon; the second concerns its chemical state, which determines the mechanism of interaction between the muon spin and the magnetic moments of the system.

In order to clarify such features in a family of magnetic insulators that have represented some sort of "model" systems in the past, antiferromagnetic crystals of MnF_2 and CoF_2 have been investigated in detail, and the findings concerning the localization of muons as well as the mechanisms of interaction have been given in the companion paper (hereafter referred to as paper I).⁸ On the basis of this information, which can be summarized by stating

that muons are localized in interstitial sites of known symmetry in both crystals, where they detect the behavior of the magnetic system via dipole-dipole interactions, it is then possible to investigate the magnetic properties of such systems as seen by implanted muons and provide a comparison with the rather abundant data available, especially from nuclear magnetic resonance and neutron scattering experiments.

This being the aim of the present work, we summarize here the principal features of MnF_2 and CoF_2 without the pretense of completeness. Both materials crystallize in a tetragonal structure of the rutile type, with similar a/c ratios of approximately 1.47; in the antiferromagnetic phase the transition-metal spins order in two sublattices, aligned parallel and antiparallel to the c axis. While the cobalt salt presents a very large anisotropy that makes it an almost ideal case of the three-dimensional (3D) Ising model, this parameter is much smaller in the case of the manganese salt which, therefore, could be closer to the Heisenberg model. The behavior of quantities that exhibit a critical divergence at the phase transition, such as the correlation length and the correlation time of the antiferromagnetic mode fluctuations, have been determined for both crystals, by means of NMR (Ref. 9) and neutron scattering measurements.^{10,11} Evaluations of the static and dynamic critical exponents from these measurements are in general agreement with the predictions of the scaling theory. Different behaviors are displayed by the two crystals: Especially from neutron scattering experiments,

the static correlations and the susceptibility for CoF_2 show a slower decrease of the critical effects with distance from T_N than do those for MnF_2 ; also, dynamic correlations exhibit differences associated with the anisotropy.

The same experimental techniques also allow determination of the spontaneous sublattice magnetization M_s and its temperature dependence.¹²⁻¹⁴ The spin-wave theory applies well to both these antiferromagnets at low temperatures. Closer to the transition the vanishing of $M_s(T)$ as $T \rightarrow T_N^-$ shows a much clearer $|T - T_N|^\beta$ dependence in MnF_2 than in CoF_2 . Neutron scattering data¹⁴ in the latter fail to show this behavior except for $|T - T_N| < 10^{-1}$ K while the power law in MnF_2 is valid for a range of several degrees. In this respect, however, the nature of the coupling between the experimental probe and the magnetic moments of the system plays an important role. For NMR on the nuclei of the magnetic ion this coupling is the contact hyperfine interaction and the pseudo dipolar interaction; for NMR on the ^{19}F nuclei it is the transferred hyperfine interaction due to the superexchange; in neutron scattering it is the atomic magnetic scattering factor. All these couplings, in particular, for complex ground states of the ions, such as for Co^{2+} , may vary in magnitude as the population of the nearest-excited Kramers doublet increases with temperature. In these cases the measured quantities display a behavior which is the result of the convolution of two distinct temperature-dependent factors—the relevant physical quantity and the interaction with the probe. Here μSR experiments, in addition to providing a possible confirmation of already established information, can be particularly valuable in yielding a more direct measurement of the magnetic properties of the system, if the muon coupling to the system, as suggested by its dipole-dipole nature previously determined,⁸ is free from such a problem.

In Sec. II we report on a set of measurements in CoF_2 in which M_s was determined. μSR results are therein compared to the spin-wave theory and to the $|T - T_N|^\beta$ law close to T_N .

Section III is devoted to the critical damping of the μSR signal in the neighborhood of the Néel temperature for both crystals. Correspondence to the NMR critical broadening of the linewidth and to the slowing down of the antiferromagnetic mode fluctuations is established. Further comments and discussions are included in Sec. IV.

II. TEMPERATURE DEPENDENCE OF THE SUBLATTICE MAGNETIZATION IN CoF_2

Since CoF_2 is antiferromagnetic in the ordered phase, a μSR signal in zero applied field is best seen when the following experimental geometry is respected: (a) the c axis of the crystal is orthogonal to the incoming muon-beam polarization, and (b) the positron telescopes are in the forward-backward geometry. In these conditions the μSR spectrum is characterized by one well-defined frequency, which represents the precession of the muon spin around the internal magnetic field at the site of localization. The

existence of a single frequency demonstrates the uniqueness of the site: Due to the presence of two magnetic sublattices, though, two families of muons are determined, which precess in opposite directions. This is further confirmed by the line splitting induced by an external magnetic field, as discussed in Ref. 8. In this case the value of the field produced by the sublattice magnetization, \vec{B}_{hf} (where hf represents hyperfine), in the presence of an external field \vec{B}_0 is simply given by

$$|\vec{B}_{\text{hf}}| = \left[\frac{\nu_1^2 + \nu_2^2}{2\gamma_\mu^2} - B_0^2 \right]^{1/2}, \quad (1)$$

where ν_1 and ν_2 are the two observed frequencies and γ_μ is the gyromagnetic ratio for the muon. Both measurements in zero field and in an external field yield the value of

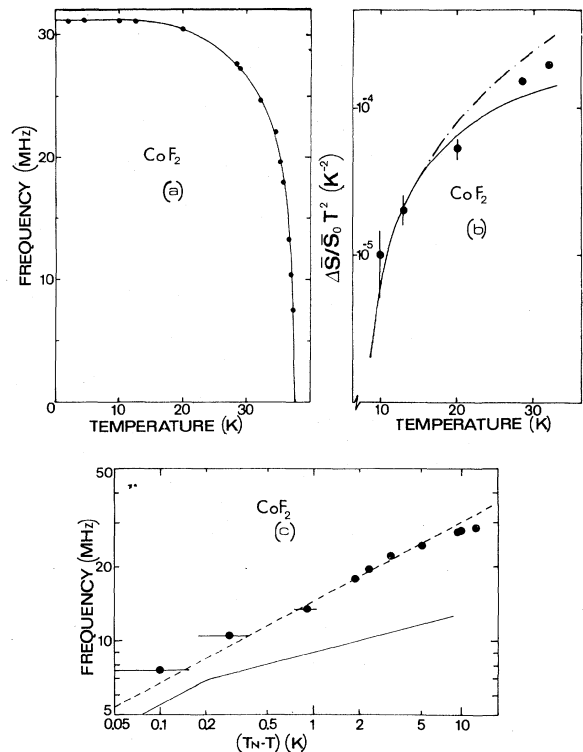


FIG. 1. Behavior of the μSR frequency versus temperature in CoF_2 in zero field is shown in (a); it is proportional to the spontaneous sublattice magnetization. In (b) the deviation of the spin $\Delta\bar{S}$ from its value at $T=0$, \bar{S}_0 , is plotted as a function of temperature. For μSR data $\Delta\bar{S}/\bar{S}_0 = \Delta\nu_\mu/\nu_\mu(T=0)$. The continuous line is the theoretical spin-wave estimate from Lines (with no exchange between spins of the same sublattice and with z_2J_2 , the effective exchange field, equal to 35 cm^{-1}). The dashed line represents NMR experimental results from Jaccarino (private communication to Lines). In (c) the data closer to the critical point are plotted in a double logarithmic scale, as a function of $T_N - T$: The line represents a fit with a slope of 0.33 ± 0.02 , consistent with the predictions of the 3D Ising model; deviation from the linear behavior appears for $T_N - T > 5$.

2288 G for B_{hf} at 2 K. It is worth recalling that the muons occupy the octahedral sites, as was discussed in Ref. 8.

The results of the temperature dependence of the μSR frequency in zero field are shown in Fig. 1(a). The overall behavior agrees qualitatively with the square root of the integrated elastic neutron scattering intensity for magnetic reflection (100).¹⁵ A more quantitative analysis, however, must be confined to either the lowest temperatures or to the region close to the critical point.

At low temperature, changes in the sublattice magnetization are induced by the excitation of spin waves. Figure 1(b) shows the spin deviation $\Delta\bar{S}$ from its value \bar{S}_0 at $T=0$ calculated directly from the muon frequency measurements:

$$\frac{\Delta\bar{S}(T)}{\bar{S}_0} = \frac{\nu_\mu(T) - \nu_\mu(T=0)}{\nu_\mu(T=0)}. \quad (2)$$

The solid line is the theoretical spin-wave estimate of the same quantity from Ref. 16. This curve was calculated on some basic assumptions, the most relevant of which are that (a) the actual antiferromagnetic ground state is sufficiently close to the molecular-field ground state for the former to be described in terms of excitations from the latter, keeping only terms up to those quadratic in the operators representing spin deviations, (b) the exchange between spins of the same sublattice is neglected ($J_1=0$), and (c) the effective exchange field is $z_2J_2=35 \text{ cm}^{-1}$. The conditions (b) and (c) were selected among similar curves with different values of J_1 and J_2 because of the close agreement with the experimental results from nuclear resonance experiments,¹⁷ which are represented in the same figure by a dashed line. The μSR data between 2 and 5 K are not reported in Fig. 1(b) because the error in $\Delta\nu_\mu/\nu_\mu T^2$ exceeds the value of the ratio itself. Up to 20 K the present data agree with the spin-wave calculation, while for higher temperature they induce larger spin deviations. As pointed out in Ref. 16 this is expected in view of the theoretical assumptions.

When the Néel temperature is approached from below, the sublattice magnetization decreases and, eventually, vanishes at T_N . The measured μSR frequency also exhibits this behavior as may be seen in Fig. 1(c). On a double logarithmic scale, as a function of $T_N - T$, the data indicate a linear behavior with systematic deviations for $T_N - T > 5 \text{ K}$. The line drawn as a reference has a slope of $\frac{1}{3}$, while the data better fit a power law with exponent $\beta=0.3$. This is quite close to the exponent predicted for the 3D Ising model, $\beta=0.31$, which is consistent with the large uniaxial anisotropy of CoF₂. For comparison, the neutron Bragg scattering experiments¹⁴ are clearly non-linear in the same temperature region as indicated by the continuous line in Fig. 1(c). A fitting to a power law was attempted only in the limited temperature interval for $T_N - T < 0.3 \text{ K}$ with the result $\beta=0.305$ also in accordance with the theoretical result for the 3D Ising model. It must be noted that, for systems such as MnF₂, neutron scattering as well as NMR measurements of the critical exponent β cover the range of several degrees from T_N , which is the case also for the present μSR data on CoF₂.

III. μSR LINEWIDTH IN THE REGION OF THE MAGNETIC PHASE TRANSITION

A. Experimental details

The characteristics of the μSR signals undergo abrupt changes across the phase transition: In particular the frequency shows a discontinuity since the free Larmor precession in the paramagnetic phase disappears below T_N . Also the precession frequency in the hyperfine field below T_N vanishes at the critical point. Both features have been exploited in the present experiment, in order to determine the values of T_N for MnF₂ and CoF₂. These agree with the values known from other experiments (67.336 K for MnF₂ from NMR data^{9,12} and 37.85 K for CoF₂ from neutron scattering data¹¹) within the tolerance of the uncalibrated platinum resistors (100 Ω) installed in our cryostats. The precision of the relative temperature measurements in the present μSR results is $\pm 0.01 \text{ K}$ at best.

The experiments in the paramagnetic phase have been performed in the presence of an external field of 3 kG, while in the antiferromagnetic region all the data were taken in zero applied field. The fitting of all data was performed under the assumption of a Lorentzian profile, which is certainly reasonable in the critical region. Sufficiently far from T_N , where exchange narrowing is most effective, the deconvolution of a Lorentzian and a Gaussian profile indicated that the latter was significant, as expected from the contributions of the nuclear dipole moments. When the field was applied perpendicular to the c axis the μSR frequency was split, as discussed in detail in paper I; in this case both lines were fitted at the same time by assuming a common linewidth. Very close to T_N , where the broadening exceeds the line splitting, a single-frequency fitting was used.

B. Dipolar fields and related properties of the linewidth

The linewidth of the precession frequency of the muon spin localized in a well-defined interstitial lattice site is determined by the characteristics of the local perturbing magnetic field $\vec{h}(t)$. In very general terms one can refer to the Moriya expression¹⁸ for the linewidth $\delta\nu^z$:

$$\delta\nu^z = \frac{\gamma^2}{2} \int_0^\infty dt \{ \langle [h_z(t)h_z(0)] \rangle + \frac{1}{2} \langle [h_x(t)h_x(0) + h_y(t)h_y(0)] \rangle \cos\omega_L t \}, \quad (3)$$

where, since the muon Larmor frequency ω_L is always much smaller than the characteristic frequency of the electron-spin dynamics, we can approximate the cosine to 1 and we will refer here to either the Co- and Mn-ion magnetic moments as the principal source for $\vec{h}(t)$. In strict analogy to nuclear magnetic resonance, when the coupling between the lattice magnetic moments and the probe is an isotropic hyperfine (or transferred hyperfine) interaction, it is possible to express the linewidth in terms

of the scattering function of the magnetic system¹⁹ $\mathcal{F}(\vec{k}, \omega)$:

$$\delta\nu^2 \cong \frac{1}{2} \left[\frac{A}{\hbar} \right]^2 \frac{1}{N} \sum_{\vec{k}} \{ \mathcal{S}^{zz}(\vec{k}, 0) + \frac{1}{2} [\mathcal{S}^{xx}(\vec{k}, 0) + \mathcal{S}^{yy}(\vec{k}, 0)] \}. \quad (4)$$

When the critical dynamics is accounted for within the slowing-down approximation, and the scattering function is expressed in terms of the wave-vector-dependent susceptibility $\chi(\vec{k})$ and of the inverse lifetime of the fluctuation of wave vector \vec{k} $\Gamma(\vec{k})$, one can write

$$\mathcal{S}(\vec{k}, 0) \propto \frac{\chi(\vec{k})}{\Gamma(\vec{k})} \propto \chi^2(\vec{k}). \quad (5)$$

$\chi(\vec{k})$ and $\Gamma(\vec{k})$ are essential quantities and have been the object of extensive theoretical calculations as well as experimental tests.¹⁹⁻²¹

For muons localized in interstitial sites in the crystals studied here, $\vec{h}(t)$ is the dipole field produced, in principle, by all the magnetic moments in the lattice, rather than by a single neighboring magnetic moment, as is generally the case for NMR experiments in magnetic insulators. In view of this qualitative difference in the coupling mechanism that produces $\vec{h}(t)$, we will examine here the circumstances in which the μ SR linewidth can be still related in a simple form to the fundamental quantities $\chi(k)$ and $\Gamma(k)$. Let us first of all introduce the local field produced by the electron spins, surely predominant in the critical region:

$$h_\alpha(t) = \sum_{i=1}^N \hbar \gamma_e \frac{3[\vec{S}_i(t) \cdot \vec{r}_i] r_i^\alpha - r_i^2 S_i^\alpha(t)}{r_i^5} \\ \cong \sum_{i,\beta} D_{\alpha\beta}(\vec{r}_i) S_i^\beta(t), \quad (6)$$

where α and β are the indices of the Cartesian components, $\vec{S}_i(t)$ is the i th electron-spin operator, \vec{r}_i is its position with respect to the muon, and \vec{D} is thus defined as the dipolar tensor. Therefore, the correlation function of the local fields \vec{h} can again be expressed in terms of the spin-correlation function $\vec{G}(\vec{r}_i - \vec{r}_j, t)$, which depends only on the difference of the two coordinates because of the translational invariance of the system:

$$\langle [h_\alpha(t) h_\alpha(0)] \rangle = \sum_{\substack{i,j \\ \beta,\gamma}} D_{\alpha\beta}(\vec{r}_i) D_{\alpha\gamma}(\vec{r}_j) \langle [S_i^\beta(t) S_j^\gamma(0)] \rangle \\ \cong \sum_{\substack{i,j \\ \beta,\gamma}} D_{\alpha\beta}(\vec{r}_i) D_{\alpha\gamma}(\vec{r}_j) G^{\beta\gamma}(\vec{r}_i - \vec{r}_j, t). \quad (7)$$

It is convenient to express these quantities in terms of their Fourier transforms in space, following the usual scheme.¹⁹ Thus, if \mathcal{G} is the transform of \vec{G} and \mathcal{D} that

of \vec{D} , we obtain

$$\langle [h_\alpha(t) h_\alpha(0)] \rangle = \frac{1}{N} \sum_{\vec{k}} \mathcal{D}_{\alpha\beta}(\vec{k}) \mathcal{D}_{\alpha\gamma}(-\vec{k}) \mathcal{G}^{\beta\gamma}(\vec{k}, t). \quad (8)$$

The temporal Fourier transform of $\mathcal{G}(\vec{k}, t)$ coincides, for practical purposes, with the scattering function $\mathcal{F}(\vec{k}, \omega)$. Let us now consider expression (8) in the region very close to T_N and translate the origin of the Brillouin zone to the antiferromagnetic point \vec{k}_0 ($\vec{q} = \vec{k} - \vec{k}_0$), where \vec{k}_0 is such that $\exp(-i\vec{k}_0 \cdot \vec{r}_i)$ takes the value $+1$ on one sublattice and -1 on the other. Since for $T \rightarrow T_N$ the fluctuations at wave vector $\vec{q} = 0$ increase in amplitude and become increasingly slower, we can assume that the predominant contributions to expression (8) come from a small volume around $\vec{q} = 0$ whose linear dimensions are of the order of the inverse correlation length κ . In such a region the factor $\mathcal{D}(\vec{q})$ is only weakly dependent on \vec{q} and can be approximated with a constant $\mathcal{D}_0 = \mathcal{D}(0)$. This can be seen as a consequence of the fact that, on approaching T_N , the dipolar sums in (6) are nearly equal to their antiferromagnetic value as soon as the correlation length κ^{-1} becomes larger than the "convergence radius" of the sum. Besides, for the site occupied by the muon, \mathcal{D}_0 has the c axis as one of its principal axes.

We can further consider that, not only for CoF_2 , but also for MnF_2 , if we restrict ourselves to a region sufficiently close to T_N , the spin fluctuations are polarized along the c axis (i.e., \mathcal{S}^{cc} is much larger than all the other components of \mathcal{S}). As a consequence the spin fluctuations produce fluctuating magnetic fields at the muon site which are themselves along the same axis. By using these properties to evaluate (8) and with the help of (3) one obtains, for temperatures sufficiently close to T_N , the following expressions for the μ SR linewidth:

$$\delta\nu^c = \frac{1}{4} \frac{\mathcal{D}_0^{cc^2}}{N} \sum_{\vec{q}} \mathcal{S}^{cc}(\vec{q}, \omega=0), \quad (9a)$$

$$\delta\nu^a \cong \frac{1}{4} \frac{\mathcal{D}_0^{cc^2}}{N} \sum_{\vec{q}} \frac{1}{2} \mathcal{S}^{cc}(\vec{q}, \omega=0) = \frac{\delta\nu^c}{2}. \quad (9b)$$

In addition to the region very close to T_N , the interpretation of the μ SR linewidth can be particularly simple also at high temperatures, while in an intermediate region the complexity of the roles of the dipolar coupling and of the intrinsic fluctuations of the magnetic system make the analytical expression for the linewidth difficult to compare to experimental data.

When the magnetic moments are uncorrelated, i.e., for $T \gg T_N$, one expects that the magnetic fluctuations have amplitudes and lifetimes independent of the orientation and one can predict the angular dependence of $\delta\nu$ as a pure consequence of the tensorial character of the dipolar coupling. Under these conditions, as a matter of fact, the correlation functions of the local fields are given, in the extreme narrowing approximation, by

$$\langle [h_\alpha(t) h_\alpha(0)] \rangle = \langle h_\alpha^2 \rangle e^{-t/\tau_c}, \quad (10)$$

and the mean-square value of the instantaneous fields is

given by

$$\langle h_a^2 \rangle = (\gamma_e \hbar)^2 \frac{S(S+1)}{3} \sum_i \frac{1+3\cos^2\theta_i}{r_i^6}, \quad (11)$$

which contains all terms of the dipolar interaction. The use of (3) allows the evaluation of the linewidth and its angular dependence, provided the correlation time is known.

C. μSR linewidth data and comparison with NMR and neutron scattering

1. MnF_2

For this salt measurements were performed in the paramagnetic phase and most of the data were taken in an interval of a few degrees above T_N . Two main orientations were scanned with the external field parallel to the c axis and to the a axis.

Figure 2 shows the overall behavior of the linewidth as a function of $T - T_N$. The critical broadening is evident for both orientations and it takes place within 1 K from T_N . The inset displays the same data on a double logarithmic scale where one can see that the asymptotic behavior is consistent with a power law.

For temperatures above $T_N + 1$ K, where fluctuations are expected to be noncritical (i.e., isotropic and in the exchange-controlled regime), two essential features appear.

(i) The line shape is not a pure Lorentzian, but it can be fitted with a Gaussian-Lorentzian convolution whose contributions are represented in the inset by a square and an

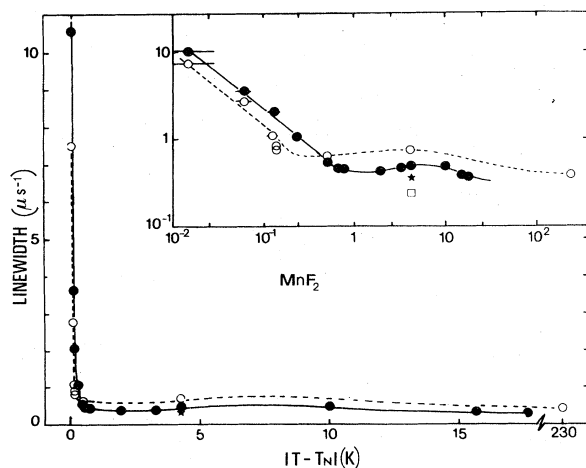


FIG. 2. Behavior of the μSR linewidth as a function of temperature for MnF_2 in an external field of 3 kG; a Lorentzian line shape was assumed. Data for two different crystal orientations are shown: with the magnetic field parallel to the c axis (closed circles) and to the a axis (open circles). The inset displays the same data on a double logarithmic scale: Here the anisotropy of the linewidth is quite evident, together with its inversion around $T_N + 0.4$ K (both lines drawn through the points are guides to the eye). The asterisk and the open square represent the Lorentzian and Gaussian components, respectively, of a deconvolution of the $T_N + 4.3$ K closed circle.

asterisk, respectively. In particular the Gaussian term of 220 ± 100 KHz must be due to the nuclear spins of the system, and it compares well with the calculated contribution of 310 KHz under the assumption that the muon is at rest, as we know to be the case. The Lorentzian contribution remains, however, the largest, and its value at $T_N + 4$ K is 500 KHz.

(ii) As expected, the angular dependence of the linewidth reflects the tensorial character of the dipolar fields; in particular $\delta\nu^c/\delta\nu^a=0.7$. By using expression (11) for the dipolar sums with the muon in the octahedral sites, one obtains the value 0.83 for the same ratio.

Upon approaching T_N , one observes an inversion in the linewidth anisotropy: within 10^1 K from T_N $\delta\nu^c$ becomes larger than $\delta\nu^a$ and their ratio is 1.6. In this region the anisotropy of the fluctuations is responsible for a value of the ratio of 2, as predicted by (9a) and (9b) and as experimentally observed in NMR in the same crystal.^{9,19} In NMR, though, the inversion was not observed owing to the isotropic character of the coupling mechanism. One can then realize that the dipolar character of the interaction with the muon offers a simple way to "recognize" the beginning of the critical region. The temperature at which the crossover takes place, which is near $T_N=0.4$ K, seems easier to identify than the slow merging of two curves.

The divergence of the linewidth is approximated by a power law with an exponent of 0.8 ± 0.2 . The predictions for the 3D Heisenberg and Ising models for both the NMR and μSR linewidth exponent n are compatible with this value and, because of the experimental error on n , one cannot distinguish between the two models. On the other hand, the Ising model should be more appropriate, in consideration of the evident anisotropy of the fluctuations described above. In a comparison with the existing NMR data on the same material,⁹ one notes that the latter indicate a severe rounding off of the slope in the temperature region below $T_N + 0.01$ K; due to the large size of our sample, the length of the data taking and the overall performance of the cryogenic system, our data cannot cover the same temperature range. It should be pointed out, however, that the beginning of the rounding off is not evident in the trend of the μSR data.

2. CoF_2

In addition to the linewidth divergence in the paramagnetic region, in CoF_2 it was possible to determine the corresponding phenomenon when approaching T_N from the antiferromagnetic phase. Figure 3 reports the μSR data for the linewidth versus $T - T_N$: The data above T_N were taken with an external field of 3 kG applied parallel to the crystal c axis, while the data below T_N are the linewidths of the precession frequency around the spontaneous hyperfine field (see Fig. 1) in zero external field. The inset displays the same data on a double logarithmic scale and the dotted line represents the power law with slope $\frac{2}{3}$. In the paramagnetic region the data are well approximated by a power law with an exponent equal to $\frac{2}{3}$, as expected for this highly anisotropic crystal; the data represented by open circles are the Lorentzian components of the

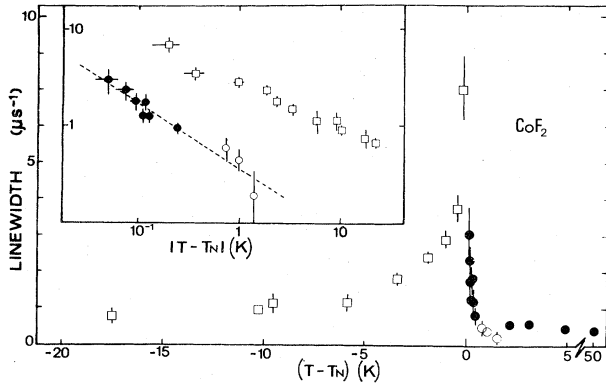


FIG. 3. Linewidths for CoF_2 versus $T - T_N$: closed circles represent the data relative to the free Larmor precession above T_N around an external magnetic field of 3 kG applied along the c axis; open circles represent the Lorentzian component of a Gaussian-Lorentzian convolution. Open squares are relative to the precession in zero applied field, around the local hyperfine field due to the spontaneous magnetization. The inset shows the same data on a double logarithmic scale and the dashed line corresponds to a slope $n = \frac{2}{3}$.

linewidth, as deconvoluted from the experimental profile. The remaining Gaussian component for the same points was 400 ± 100 KHz, which agrees with the value of 360 KHz calculated for the nuclear dipolar contribution on a muon at rest in an octahedral site. The behavior of the data in the paramagnetic phase is therefore consistent with that accounted for by the “slowing-down” approximation (5), since the critical exponent $\frac{2}{3}$ is a direct result of the q summation of the square of the wavevector—dependent susceptibility.²²

The data below T_N show two important differences: Firstly, the slope is not as well defined as it is above T_N and, when all data are approximated with a single straight line, its slope is close to 0.5; secondly, the absolute values of the linewidth are consistently larger than that above T_N , with an average ratio of 5.5. The assumptions of the “slowing-down” approximation are not valid in the antiferromagnetic phase, and, in order to evaluate $\mathcal{S}(\vec{q}, 0)$ one must estimate independently the behavior of $\chi(\vec{q})$ and $\Gamma(\vec{q})$. It is thus not surprising to find a different linewidth factor in this phase. On the other hand, the basic assumption of the scaling theory is that the critical behavior must be the same above and below T_N , which amounts to stating that one expects equal critical exponents. The range of reduced temperatures where this holds true, though, does not necessarily coincide on the two sides of the critical point. In this respect it is important to note that the experimental resolution precludes a closer approach to T_N from below: Our data are probably not fully in the asymptotic region.

IV. DISCUSSION AND CONCLUSIONS

While the general features of the muon as a probe have been presented and discussed in paper I, the present μSR

experiments concern the intrinsic magnetic properties of the two different antiferromagnets. Some aspects of our data allow a straightforward interpretation and confirm features known from other experiments. Other aspects help to clarify important points where other techniques seem to give incomplete results, such as the critical vanishing of the magnetization close to T_N in CoF_2 and some details of the critical dynamics in the ordered phase.

At low temperatures the variation of sublattice magnetization as monitored by μSR agrees with both the theoretical spin-wave predictions and the experimental determination of the NMR frequency in CoF_2 ; close to T_N the data on the sublattice magnetization also presented in Sec. II follow the expected $T - T_N$ to the $\frac{1}{3}$ law without the deviations observed in neutron scattering data for the same material.¹⁴ Without the pretense of reinterpreting the neutron scattering data, whose deviations from the $\frac{1}{3}$ law were attributed by the authors to problems of extinction in a large single crystal, the possible temperature dependence of the coupling between the neutrons and the magnetic lattice, i.e., the square modulus of $f(\vec{q})$ in Ref. 14, needs to be given more consideration. In contrast with this, the coupling between the spontaneous magnetization and the muon is the temperature-independent dipolar tensor \vec{D} , and therefore the clear $\frac{1}{3}$ law in the μSR data provides a straightforward confirmation of the expected critical behavior.

Among the various aspects of the μSR linewidth behavior for MnF_2 , the inversion of the ratio $\delta v^e / \delta v^a$ at $T - T_N = 0.4$ K deserves a few comments. This inversion characterizes the transition from a regime of isotropic fluctuations, far from T_N , where the residual anisotropy is due solely to the tensorial character of the dipolar coupling, to a regime of highly anisotropic fluctuations, closer to T_N . The crossover between the two regimes was already invoked in the discussion of NMR data⁹ and specific-heat measurements,²³ where the continuous change in the scaling functions of the linewidth and the magnetic specific heat, respectively, takes place in a region around the crossover temperature. This temperature, T_X , defined²³ as

$$(T_X - T_N) / T_N \equiv |H_a / H_e|^{1.25}, \quad (12)$$

where H_a and H_e are the anisotropy and exchange fields, respectively, corresponds to a value of 0.26 or 0.54 K in $T - T_N$, depending on whether the dipolar or the crystal-field anisotropy interaction is used. The sharp change shown by our data just in between these two temperatures is a very clear signature of the crossover, which therefore supports the explanation of the more gradual variations measured with the other two techniques.

Further comments are needed for the data in the interval $T_N < T < T_X$: Here, on the basis of the discussion of Sec. III A, a comparison can be made with the critical divergence of the ^{19}F NMR linewidth.⁹ Besides the agreement on the value of the critical exponents found in the two cases, one could attempt to compare directly the magnitudes of the two linewidths. When sufficiently close to the Néel point one can roughly approximate expression (9a) by

$$\delta\nu^c = \omega_0^2 \tau_c / 2\pi, \quad (13)$$

where ω_0 is the precession frequency around the instantaneous local field at the probe and τ_c is the correlation time of this field. By further assuming that τ_c is the same both for the field at the muon site and for that at the ¹⁹F site—which seems reasonably very close to T_N —one obtains a rough estimate of the antiferromagnetic field at the muon site as

$$H_{\text{hf}}^\mu(T=0) \cong \frac{\gamma_F}{\gamma_\mu} \left[\frac{\delta\nu_\mu^c}{\delta\nu_F^c} \right]^{1/2} H_{\text{hf}}^F(T=0). \quad (14)$$

This gives a value of 13 kG, which is larger than expected for the supposed site of occupancy of the muon (4.5 kG at the octahedral site), and it would agree better with the prediction for the fluorinelike tetrahedral⁸ (12.5 kG) site. This conclusion, however, cannot be drawn too rigorously in view of the oversimplifications involved in Eq. (14).

One of the most interesting features of the μ SR linewidth in CoF₂ is the asymmetry in the two regimes above and below T_N , presented in Sec. III A 2. The line broadening below T_N begins at a larger distance from T_N than above it. Its temperature dependence is clearly critical and this corresponds to the existence of the significant central peak in the $\mathcal{S}(\vec{q}, \omega)$, familiar in neutron scattering, which narrows critically as T_N is approached. The validity of scaling theories implies the same critical exponents in both regimes, and this symmetry emerges only as a trend in the μ SR data below T_N where, as discussed in Sec. III A 2, too large a broadening prevented the investigation of the really asymptotic region. A second important feature is the absolute value of the μ SR linewidth, which is much larger below than above T_N ($\delta\bar{\nu}/\delta\nu^+ = 5.5$), which obviously implies that the nature of the central peak is more complex than in the paramagnetic regime. As a matter of fact, below T_N the shape of the scattering function is modified by the characteristic spin-wave side peaks, which “soften” and collapse at $\omega=0$ for $T=T_N$. The scaling theory predicts precise values for the ratios χ^+/χ^- and κ^+/κ^- (nearly 5 and 1.96, respectively)²⁴ and direct confirmation comes from neutron

scattering experiments both on CoF₂ and MnF₂. Using these values to interpret our μ SR linewidth data, we must conclude that the corresponding ratio for the width Γ of the central peak is $\Gamma^+\Gamma^- = 4$, which means that the scattering function is systematically narrower below T_N than above it. Neutron scattering has so far failed to provide information regarding the low frequency and low \vec{q} features of $\mathcal{S}(\vec{q}, \omega)$ in CoF₂, and therefore the present μ SR results are, as far as we know, the only indication of the dynamic properties of the central peak below T_N in CoF₂. For MnF₂, on the other hand, the phenomenology from NMR and neutron scattering is more complete: The experimental values for $\Gamma(\vec{q})$ at low \vec{q} are considerably smaller below than above T_N , and NMR linewidth measurements revealed an asymmetry similar to the μ SR data in the two temperature regimes. The idea of a diffusive central peak below T_N in MnF₂, consistent with such experiments, is supported by theoretical considerations²⁵ as well as by thermodynamical arguments.¹⁹ It seems therefore quite plausible that the μ SR linewidth in CoF₂ reflects the same type of phenomenon in the critical region since the magnetic Hamiltonians for the two crystals are qualitatively the same.

ACKNOWLEDGMENTS

The authors appreciated the assistance of Dr. T. Niinikoski and Mr. G. Coubra of the Polarized Target Group at CERN for the low-temperature equipment, the constant attention of the CERN Synchrocyclotron Machine (MCS) Group to the beam-related problems of the experiments, the collaboration of the personnel of the x-ray division of the National Research Council (CNR) Maspec Laboratory for the single-crystal orientations, and the valuable comments and suggestions of Professor L. Reatto. This work was supported by the Consiglio Nazionale delle Ricerche, Rome, and by the Experimental Physics Division of CERN, Geneva. Part of the experimental equipment was supported by Istituto Nazionale di Fisica Nucleare (INFN) Milan. One of us (R.D.R.) gratefully acknowledges partial support for the present work granted by Rutherford Appleton Laboratory (Oxfordshire).

- ¹A. B. Denison, H. Graf, W. Kuendig, and P. F. Meier, *Helv. Phys. Acta* **52**, 460 (1979).
- ²K. J. Rugg, C. Boekema, A. B. Denison, W. P. Hofmann, and W. Kuendig, *J. Magn. Magn. Mater.* **15–18**, 669 (1980).
- ³E. Holzschuh, C. Boekema, W. Kuendig, K. J. Rugg, and B. D. Patterson, *Hyperfine Interactions* **8**, 615 (1981).
- ⁴Y. J. Uemura, T. Yamazaki, Y. Kitaoka, M. Takigawa, and H. Yasuoka, *Hyperfine Interactions* **17**, 339 (1984).
- ⁵R. De Renzi, R. Tedeschi, G. Guidi, C. Bucci, and S. F. J. Cox, *Solid State Commun.* **43**, 683 (1982).
- ⁶C. Boekema, *Philos. Mag.* **B 42**, 409 (1980).
- ⁷E. Holzschuh, W. Kuendig, and A. B. Denison, *Hyperfine Interactions* **17**, 345 (1984).
- ⁸R. De Renzi, G. Guidi, P. Podini, R. Tedeschi, C. Bucci, and

- S. F. J. Cox, preceding paper, *Phys. Rev. B* **30**, 186 (1984).
- ⁹P. Heller and G. B. Benedek, *Phys. Rev. Lett.* **8**, 428 (1962).
- ¹⁰M. P. Schulhof, P. Heller, R. Nathans, and A. Linz, *Phys. Rev. B* **4**, 2254 (1971).
- ¹¹R. A. Cowley, W. J. L. Buyers, P. Martel, and R. W. H. Stevenson, *J. Phys. C* **6**, 2997 (1973).
- ¹²P. Heller, *Phys. Rev.* **146**, 403 (1966).
- ¹³V. Jaccarino, *Phys. Rev. Lett.* **2**, 163 (1959).
- ¹⁴R. A. Cowley and E. K. Carneiro, *J. Phys. C* **13**, 3281 (1980).
- ¹⁵P. Martel, R. A. Cowley, and R. W. H. Stevenson, *Can. J. Phys.* **46**, 1355 (1968).
- ¹⁶M. E. Lines, *Phys. Rev.* **137**, A982 (1965).
- ¹⁷V. Jaccarino, in a private communication to M. E. Lines.
- ¹⁸T. Moriya, *Prog. Theor. Phys.* **28**, 371 (1962).

- ¹⁹P. Heller, in *Local Properties at Phase Transitions*, edited by K. A. Mueller and A. Rigamonti (North-Holland, Amsterdam, 1976), p. 447.
- ²⁰M. E. Fisher and R. J. Burford, *Phys. Rev.* **156**, 587 (1967).
- ²¹B. I. Halperin and P. C. Hohenberg, *Phys. Rev.* **177**, 952 (1969).
- ²²C. Bucci and G. Guidi, *Phys. Rev. B* **9**, 3053 (1974).
- ²³N. Akutsu and H. Ikeda, *J. Phys. Soc. Jpn.* **50**, 2865 (1981).
- ²⁴H. B. Tarko and M. E. Fisher, *Phys. Rev. B* **11**, 1217 (1975).
- ²⁵B. I. Halperin and P. C. Hohenberg, *Phys. Rev.* **188**, 898 (1969).